A reconstruction strategy in 3D Compton scattering imaging

Gaël Rigaud

Institute of Mathematics
University of Würzburg, Germany

Conference on **Modern Challenges in Imaging**
In the Footsteps of Allan MacLeod Cormack

Julius-Maximilians-
UNIVERSITÄT
WÜRZBURG

The Radon transform over a family of curves – A.M. Cormack

A.M. Cormack (1981) The Radon Transform on a Family of Curves in the Plane, Proceedings of the American Mathematical Society, Vol. 83, No. 2, pp. 325-330.

Cormack

- studied the Radon transform along α and β curves:

$$\mathfrak{C}_\alpha(p,\varphi) = \left\{ x = (r,\theta) \in \mathbb{R}^2 \ : \ r^\alpha \cos(\alpha(\theta-\varphi)) = p^\alpha, \ |\theta-\varphi| \leq \pi/2\alpha \right\}$$

$$\mathfrak{C}_\beta(p,\varphi) = \left\{ x = (r,\theta) \in \mathbb{R}^2 \ : \ p^\beta \cos(\beta(\theta-\varphi)) = r^\beta, \ |\theta-\varphi| \leq \pi/2\beta \right\}$$

  which extend the straight lines (case $\alpha = 1$) considered for the standard Radon transform.
- and proved an inversion formula in the circular harmonic domain.

$\alpha = 1$

The Radon transform over a family of curves – A.M. Cormack

A.M. Cormack (1981) The Radon Transform on a Family of Curves in the Plane, Proceedings of the American Mathematical Society, Vol. 83, No. 2, pp. 325-330.

Cormack

- studied the Radon transform along α and β curves:

$$\mathfrak{C}_\alpha(p,\varphi) = \left\{x = (r,\theta) \in \mathbb{R}^2 \ : \ r^\alpha \cos(\alpha(\theta-\varphi)) = p^\alpha, \ |\theta-\varphi| \leq \pi/2\alpha\right\}$$

$$\mathfrak{C}_\beta(p,\varphi) = \left\{x = (r,\theta) \in \mathbb{R}^2 \ : \ p^\beta \cos(\beta(\theta-\varphi)) = r^\beta, \ |\theta-\varphi| \leq \pi/2\beta\right\}$$

  which extend the straight lines (case $\alpha = 1$) considered for the standard Radon transform.
- and proved an inversion formula in the circular harmonic domain.

$\beta = 1/2$

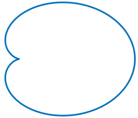

The Radon transform over a family of curves – A.M. Cormack

A.M. Cormack (1981) The Radon Transform on a Family of Curves in the Plane, Proceedings of the American Mathematical Society, Vol. 83, No. 2, pp. 325-330.

Cormack

- studied the Radon transform along α and β curves:

$$\mathfrak{C}_\alpha(p,\varphi) = \left\{ x = (r,\theta) \in \mathbb{R}^2 \ : \ r^\alpha \cos(\alpha(\theta-\varphi)) = p^\alpha, \ |\theta-\varphi| \leq \pi/2\alpha \right\}$$

$$\mathfrak{C}_\beta(p,\varphi) = \left\{ x = (r,\theta) \in \mathbb{R}^2 \ : \ p^\beta \cos(\beta(\theta-\varphi)) = r^\beta, \ |\theta-\varphi| \leq \pi/2\beta \right\}$$

  which extend the straight lines (case $\alpha = 1$) considered for the standard Radon transform.
- and proved an inversion formula in the circular harmonic domain.

$\beta = 1$

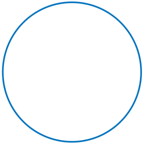

The Radon transform over a family of curves – A.M. Cormack

A.M. Cormack (1981) The Radon Transform on a Family of Curves in the Plane, Proceedings of the American Mathematical Society, Vol. 83, No. 2, pp. 325-330.

Cormack

- studied the Radon transform along α and β curves:

$$\mathfrak{C}_\alpha(p,\varphi) = \left\{ x = (r,\theta) \in \mathbb{R}^2 \ : \ r^\alpha \cos(\alpha(\theta-\varphi)) = p^\alpha, \ |\theta-\varphi| \leq \pi/2\alpha \right\}$$

$$\mathfrak{C}_\beta(p,\varphi) = \left\{ x = (r,\theta) \in \mathbb{R}^2 \ : \ p^\beta \cos(\beta(\theta-\varphi)) = r^\beta, \ |\theta-\varphi| \leq \pi/2\beta \right\}$$

  which extend the straight lines (case $\alpha = 1$) considered for the standard Radon transform.
- and proved an inversion formula in the circular harmonic domain.

$\beta = 2$

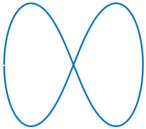

A family of circular-arcs

G. Rigaud (2013) On the inversion of the RT on a generalized Cormack-type class of curves, Inverse Problems, 29, 115010.

Definition : $\mathfrak{C}$-curves [R'13]

We define the class of curves, C by

$$\mathfrak{C}(p,\theta) = \{x : h_1(p) = h_2(x)\cdot\theta\}$$

with h_1 an odd C^∞-diffeomorphism and h_2 is a C^∞-diffeomorphic function acting on the radial component of x, $r = |x|$, with

$$h_2(r) = \left\{\frac{2sr}{r^2 - ks^2}, \frac{2sr}{1 - ks^2 r^2}\right\} \qquad s, k \in \mathbb{R}.$$

A family of circular-arcs

G. Rigaud (2013) On the inversion of the RT on a generalized Cormack-type class of curves, Inverse Problems, 29, 115010.

Definition : $\mathfrak{C}$-curves [R'13]

We define the class of curves, C by

$$\mathfrak{C}(p,\theta) = \{x : h_1(p) = h_2(x)\cdot\theta\}$$

with h_1 an odd C^∞-diffeomorphism and h_2 is a C^∞-diffeomorphic function acting on the radial component of x, $r = |x|$, with

$$h_2(r) = \left\{ \frac{2sr}{r^2 - ks^2}, \frac{2sr}{1 - ks^2 r^2} \right\} \qquad s, k \in \mathbb{R}.$$

generate circular-arcs:

Illustration in 2D : A rotation-free modality

G. Rigaud (2017) Compton Scattering Tomography: Feature Reconstruction and Rotation-Free Modality *SIAM J. Imaging Sci.*, 10(4), 2217-2249.

- S is fixed and a detector ring surronds the object.
- **Advantage:** No Rotation of the source and no collimation required

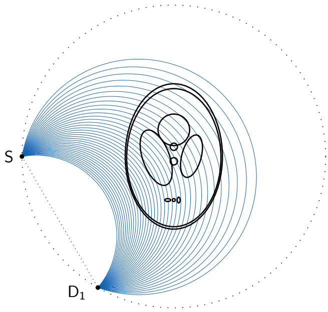

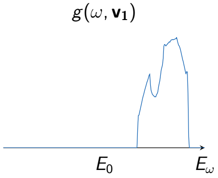

Illustration in 2D : A rotation-free modality

G. Rigaud (2017) Compton Scattering Tomography: Feature Reconstruction and Rotation-Free Modality *SIAM J. Imaging Sci.*, 10(4), 2217-2249.

- S is fixed and a detector ring surronds the object.
- **Advantage:** No Rotation of the source and no collimation required

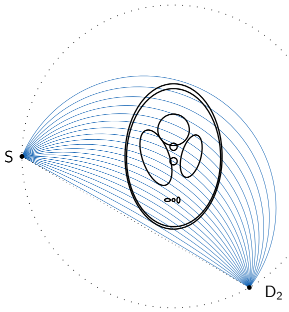

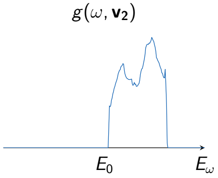

Illustration in 2D : A rotation-free modality

G. Rigaud (2017) Compton Scattering Tomography: Feature Reconstruction and Rotation-Free Modality *SIAM J. Imaging Sci.*, 10(4), 2217-2249.

- S is fixed and a detector ring surronds the object.
- **Advantage:** No Rotation of the source and no collimation required

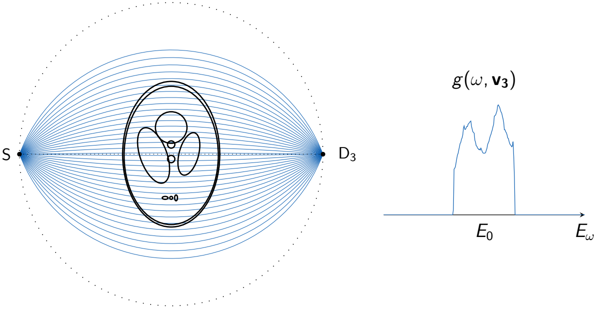

Illustration in 2D : A rotation-free modality

G. Rigaud (2017) Compton Scattering Tomography: Feature Reconstruction and Rotation-Free Modality *SIAM J. Imaging Sci.*, 10(4), 2217-2249.

- S is fixed and a detector ring surronds the object.
- **Advantage:** No Rotation of the source and no collimation required

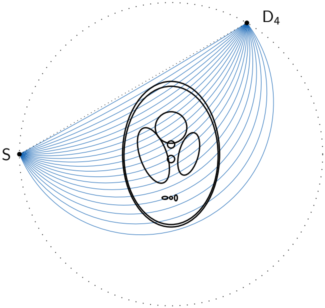

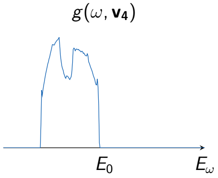

Illustration in 2D : A rotation-free modality

G. Rigaud (2017) Compton Scattering Tomography: Feature Reconstruction and Rotation-Free Modality *SIAM J. Imaging Sci.*, 10(4), 2217-2249.

- S is fixed and a detector ring surronds the object.
- **Advantage:** No Rotation of the source and no collimation required

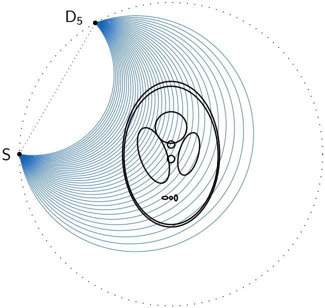

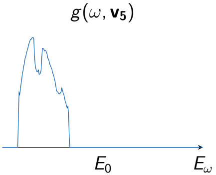

Illustration in 2D : A rotation-free modality

G. Rigaud (2017) Compton Scattering Tomography: Feature Reconstruction and Rotation-Free Modality *SIAM J. Imaging Sci.*, 10(4), 2217-2249.

- S is fixed and a detector ring surronds the object.
- **Advantage:** No Rotation of the source and no collimation required

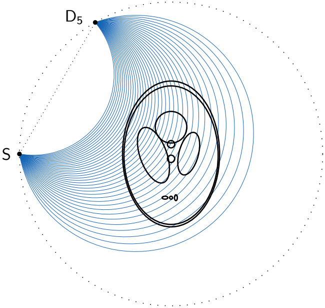

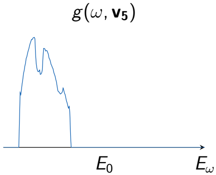

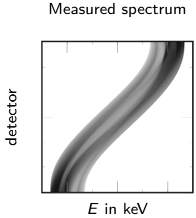

Illustration in 2D : A rotation-free modality

G. Rigaud (2017) Compton Scattering Tomography: Feature Reconstruction and Rotation-Free Modality *SIAM J. Imaging Sci.*, 10(4), 2217-2249.

- S is fixed and a detector ring surronds the object.
- **Advantage:** No Rotation of the source and no collimation required

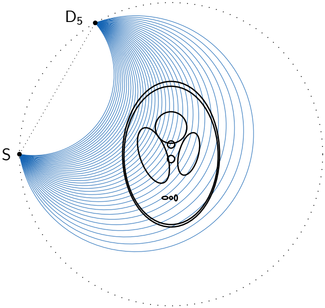

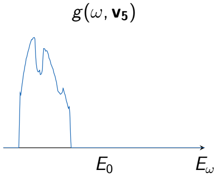

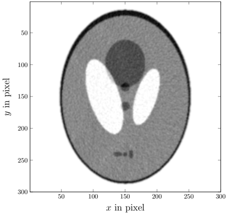

Physical interactions between photons and matter

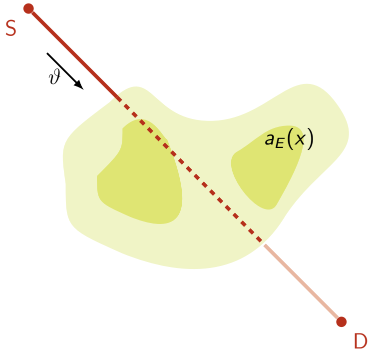

- $a_E(x)$ lineic attenuation coefficient at energy E
- $n_e(x)$ electron density

A photon beam flying in a closed domain Ω with energy E satisfies the **stationary transport equation**

$$\vartheta \cdot \nabla_x I(x, \vartheta) + a_E(x) I(x, \vartheta) = 0, \qquad x \in \Omega$$

Beer-Lambert law

$$\frac{I(D)}{I(S)} = e^{-\int_{S \to D} a_E} =: e^{-\mathcal{R} a_E}$$

The attenuation factor stands for a sum of phenomena which hinder the propagation of the traveling photons:

$$a_E(x) \approx E^{-3} \mu_{PE}(x) + \sigma(E) n_e(x)$$

- Photoelectric absorption (low energy)
- Compton scattering (high energy)

Physical interactions between photons and matter

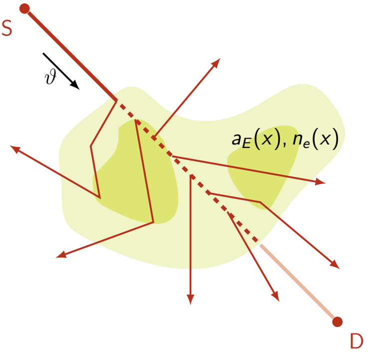

- $a_E(x)$ lineic attenuation coefficient at energy E
- $n_e(x)$ electron density

A photon beam flying in a closed domain Ω with energy E satisfies the **stationary transport equation**

$$\vartheta \cdot \nabla_x I(x,\vartheta) + a_E(x) I(x,\vartheta) = 0, \qquad x \in \Omega$$

Beer-Lambert law

$$\frac{I(D)}{I(S)} = e^{-\int_{S\to D} a_E} =: e^{-\mathcal{R}a_E}$$

The attenuation factor stands for a sum of phenomena which hinder the propagation of the traveling photons:

$$a_E(x) \approx E^{-3}\mu_{PE}(x) + \sigma(E) n_e(x)$$

- Photoelectric absorption (low energy)
- **Compton scattering** (high energy)

Compton scattering in CT

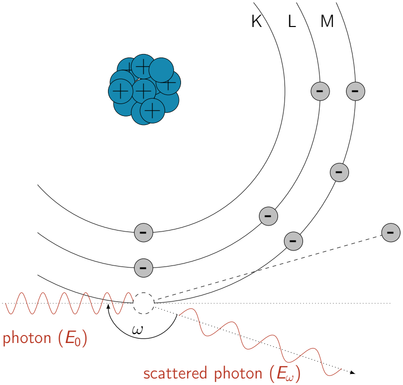

Compton Formula

$$E_\omega = \frac{E_0}{1 + \frac{E_0}{511keV}(1 + \cos\omega)}$$

Compton-Effect in CT

→ 70 to 80 % of the emitted radiation

→ treated as noise

How is it exploited today?

→ Compton camera

→ multi-energy CT

Why to use it?

→ substantial part of the radiation (>70%)

→ development of the technology of detectors

→ a new dimension to explore.

An informative spectrum

Compton Formula

$$E_\omega = \frac{E_0}{1 + \frac{E_0}{511 keV}(1 + \cos\omega)}$$

How to exploit it as imaging agent?

→ Compton scattering transforms a monochromatic spectrum (S) into a polychromatic spectrum (D).

→ Use the spectrum of the measured photons as a vector of information.

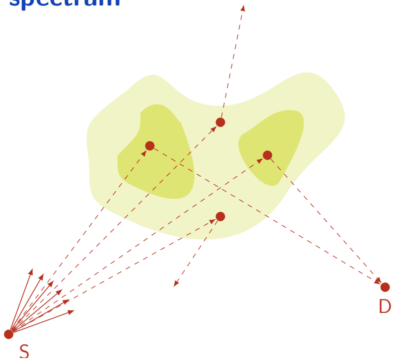

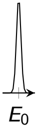

An informative spectrum

Compton Formula

$$E_\omega = \frac{E_0}{1 + \frac{E_0}{511keV}(1 + \cos\omega)}$$

How to exploit it as imaging agent?

→ Compton scattering transforms a monochromatic spectrum (S) into a polychromatic spectrum (D).

→ Use the spectrum of the measured photons as a vector of information.

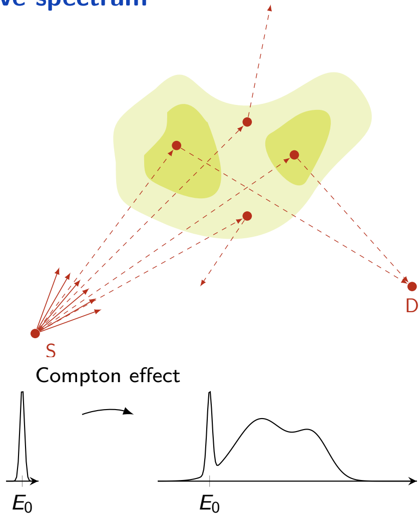

An informative spectrum

Compton Formula

$$E_\omega = \frac{E_0}{1 + \frac{E_0}{511keV}(1 + \cos \omega)}$$

How to exploit it as imaging agent?

$\longrightarrow$ Compton scattering transforms a monochromatic spectrum (S) into a polychromatic spectrum (D).

$\longrightarrow$ Use the spectrum of the measured photons as a vector of information.

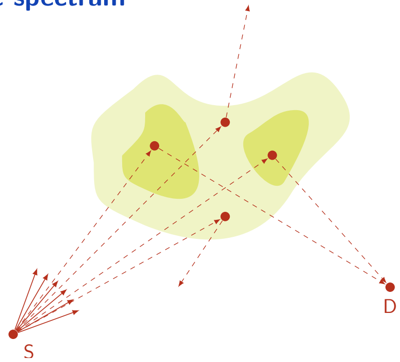

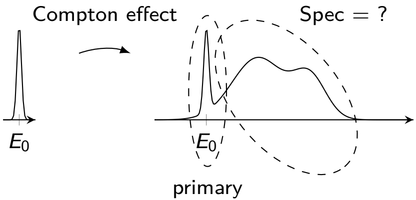

An informative spectrum

Compton Formula

$$E_\omega = \frac{E_0}{1 + \frac{E_0}{511keV}(1 + \cos\omega)}$$

How to exploit it as imaging agent?

$\rightarrow$ Compton scattering transforms a monochromatic spectrum (S) into a polychromatic spectrum (D).

$\rightarrow$ Use the spectrum of the measured photons as a vector of information.

Decomposition of the spectrum

$$\mathrm{Spec}(\mathrm{D}, E) = \sum_{i=0}^{\infty} g_i(\mathrm{D}, E).$$

with i the order of scattering.

$\Rightarrow$ $i = 1, 2$ **are the prominent cases.**

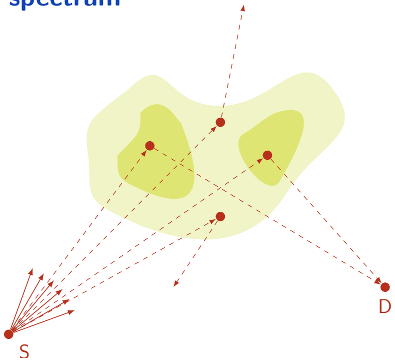

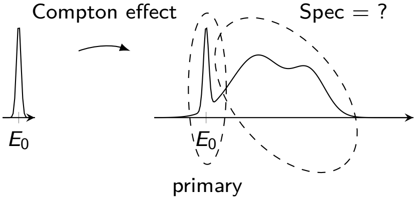

Geometry of the first-order scattered radiation

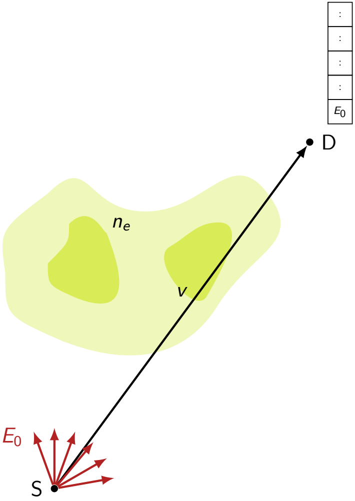

- S: monochromatic ionising source at E_0.
- D: energy-sensitive detector

Compton Formula

$$E_\omega = \frac{E_0}{1 + \frac{E_0}{511\,keV}(1 + \cos\omega)}$$

- $\mathfrak{T}(\omega, \mathbf{v}) = \{M : \widehat{SMD} = \omega\}$ stands for
  - $n = 2$ (2) circular-arc(s),
  - $n = 3$ a spindle torus.

Geometry of the first-order scattered radiation

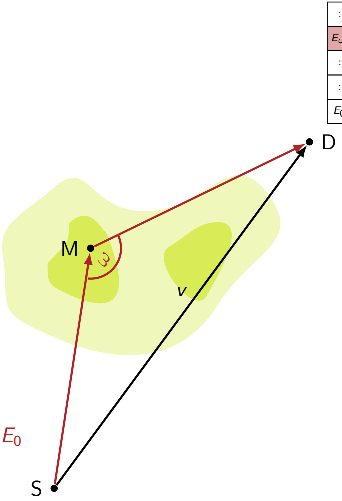

- S: monochromatic ionising source at E_0.
- D: energy-sensitive detector

Compton Formula

$$E_\omega = \frac{E_0}{1 + \frac{E_0}{511keV}(1 + \cos\omega)}$$

- $\mathfrak{T}(\omega, \mathbf{v}) = \{M : \widehat{SMD} = \omega\}$ stands for

  $n = 2$ (2) circular-arc(s),

  $n = 3$ a spindle torus.

Geometry of the first-order scattered radiation

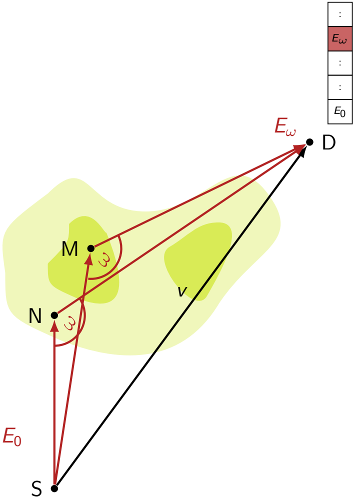

- S: monochromatic ionising source at E_0.
- D: energy-sensitive detector

Compton Formula

$$E_\omega = \frac{E_0}{1 + \frac{E_0}{511\,keV}(1 + \cos\omega)}$$

- $\mathfrak{T}(\omega, \mathbf{v}) = \{\mathrm{M} : \widehat{\mathrm{SMD}} = \omega\}$ stands for
  - $n = 2$ (2) circular-arc(s),
  - $n = 3$ a spindle torus.

Geometry of the first-order scattered radiation

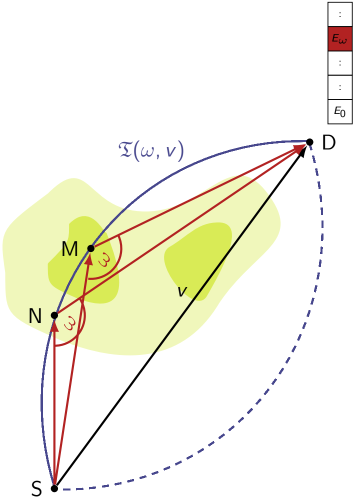

- S: monochromatic ionising source at E_0.
- D: energy-sensitive detector

Compton Formula

$$E_\omega = \frac{E_0}{1 + \frac{E_0}{511\,keV}(1 + \cos\omega)}$$

- $\mathfrak{T}(\omega, \mathbf{v}) = \{\mathrm{M} : \widehat{\mathrm{SMD}} = \omega\}$ stands for

  $n = 2$ (2) circular-arc(s),

  $n = 3$ a spindle torus.

Geometry of the first-order scattered radiation

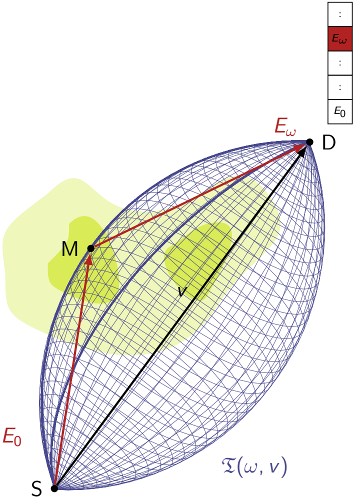

- S: monochromatic ionising source at E_0.
- D: energy-sensitive detector

Compton Formula

$$E_\omega = \frac{E_0}{1 + \frac{E_0}{511\,keV}(1 + \cos\omega)}$$

- $\mathfrak{T}(\omega, \mathbf{v}) = \{\mathrm{M} : \widehat{\mathrm{SMD}} = \omega\}$ stands for

  $n = 2$ (2) circular-arc(s),

  $n = 3$ a spindle torus.

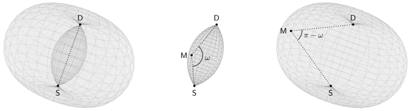

Geometry of the first-order scattered radiation

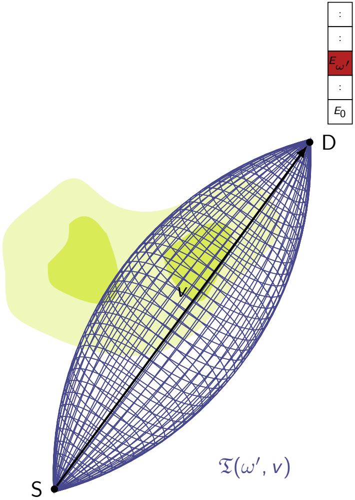

- S: monochromatic ionising source at E_0.
- D: energy-sensitive detector

Compton Formula

$$E_\omega = \frac{E_0}{1 + \frac{E_0}{511\,keV}(1 + \cos\omega)}$$

- $\mathfrak{T}(\omega, \mathbf{v}) = \{\mathrm{M} : \widehat{\mathrm{SMD}} = \omega\}$ stands for

  $n = 2$ (2) circular-arc(s),

  $n = 3$ a spindle torus.

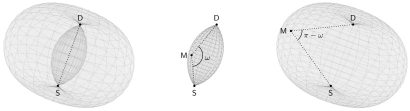

Geometry of the first-order scattered radiation

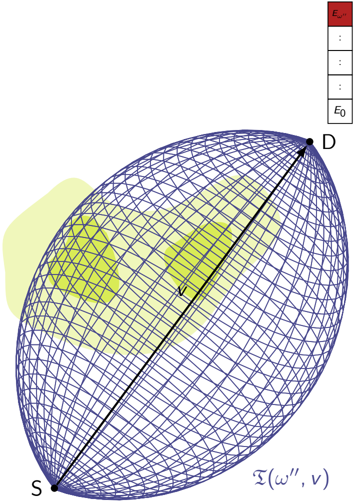

- S: monochromatic ionising source at E_0.
- D: energy-sensitive detector

Compton Formula

$$E_\omega = \frac{E_0}{1 + \frac{E_0}{511keV}(1 + \cos\omega)}$$

- $\mathfrak{T}(\omega, \mathbf{v}) = \{\mathrm{M} : \widehat{\mathrm{SMD}} = \omega\}$ stands for

  $n = 2$ (2) circular-arc(s),

  $n = 3$ a spindle torus.

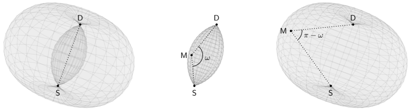

Data interpretation

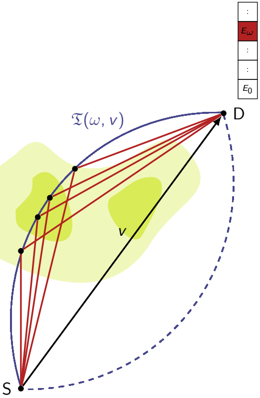

The number of photons scattered **only once** at M($\mathbf{x}$) and detected at D($\mathbf{d}$) with energy E_ω satisfies:

$$\partial_{\mathbf{x}} g_1 = \frac{I_0 r_e^2}{4} P(\omega) \frac{A_0(\mathbf{s},\mathbf{x}) A_\omega(\mathbf{x},\mathbf{d})}{\|\mathbf{s}-\mathbf{x}\|^2 \|\mathbf{x}-\mathbf{d}\|^2} n_e(\mathbf{x}) \mathrm{d}\mathbf{x},$$

with $P(\omega)$ the Klein-Nishina probability and

$$A_\omega(\mathbf{x},\mathbf{y}) = \exp\left(-\|\mathbf{y}-\mathbf{x}\| \int_0^1 a_{E_\omega} \left(\mathbf{x} + t \frac{(\mathbf{y}-\mathbf{x})}{\|\mathbf{y}-\mathbf{x}\|} \right) dt \right).$$

Assuming D to be a *point* detector,

$$g_1(\mathbf{s},\mathbf{d},\omega) \approx \int_{\mathbf{x}\in\mathfrak{T}} \frac{A_0(\mathbf{s},\mathbf{x}) A_\omega(\mathbf{x},\mathbf{d})}{\|\mathbf{s}-\mathbf{x}\|^2 \|\mathbf{x}-\mathbf{d}\|^2} n_e(\mathbf{x}) d\mathbf{x}.$$

Data interpretation

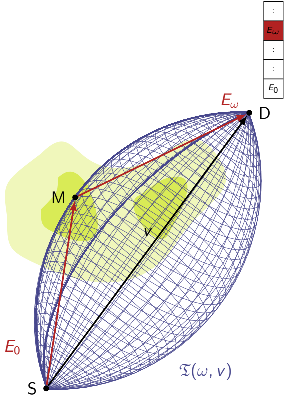

The number of photons scattered **only once** at M($\mathbf{x}$) and detected at D($\mathbf{d}$) with energy E_ω satisfies:

$$\partial_{\mathbf{x}} g_1 = \frac{I_0 r_e^2}{4} P(\omega) \frac{A_0(\mathbf{s},\mathbf{x}) A_\omega(\mathbf{x},\mathbf{d})}{\|\mathbf{s}-\mathbf{x}\|^2 \|\mathbf{x}-\mathbf{d}\|^2} n_e(\mathbf{x}) \mathrm{d}\mathbf{x},$$

with $P(\omega)$ the Klein-Nishina probability and

$$A_\omega(\mathbf{x},\mathbf{y}) = \exp\left(-\|\mathbf{y}-\mathbf{x}\| \int_0^1 a_{E_\omega} \left(\mathbf{x} + t \frac{(\mathbf{y}-\mathbf{x})}{\|\mathbf{y}-\mathbf{x}\|} \right) dt \right).$$

Assuming D to be a *point* detector,

$$g_1(\mathbf{s},\mathbf{d},\omega) \approx \int_{\mathbf{x}\in\mathfrak{T}} \frac{A_0(\mathbf{s},\mathbf{x}) A_\omega(\mathbf{x},\mathbf{d})}{\|\mathbf{s}-\mathbf{x}\|^2 \|\mathbf{x}-\mathbf{d}\|^2} n_e(\mathbf{x}) d\mathbf{x}.$$

Data interpretation

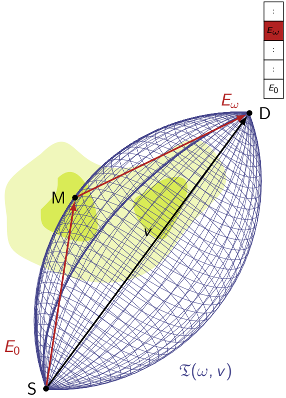

The number of photons scattered **only once** at M($\mathbf{x}$) and detected at D($\mathbf{d}$) with energy E_ω satisfies:

$$\partial_{\mathbf{x}} g_1 = \frac{I_0 r_e^2}{4} P(\omega) \frac{A_0(\mathbf{s},\mathbf{x}) A_\omega(\mathbf{x},\mathbf{d})}{\|\mathbf{s}-\mathbf{x}\|^2 \|\mathbf{x}-\mathbf{d}\|^2} n_e(\mathbf{x}) \mathrm{d}\mathbf{x},$$

with $P(\omega)$ the Klein-Nishina probability and

$$A_\omega(\mathbf{x},\mathbf{y}) = \exp\left(-\|\mathbf{y}-\mathbf{x}\| \int_0^1 a_{E_\omega}\left(\mathbf{x} + t\frac{(\mathbf{y}-\mathbf{x})}{\|\mathbf{y}-\mathbf{x}\|}\right) dt\right).$$

Assuming D to be a *point* detector,

$$g_1(\mathbf{s},\mathbf{d},\omega) \approx \int_{\mathbf{x}\in\mathfrak{T}} \frac{A_0(\mathbf{s},\mathbf{x}) A_\omega(\mathbf{x},\mathbf{d})}{\|\mathbf{s}-\mathbf{x}\|^2 \|\mathbf{x}-\mathbf{d}\|^2} n_e(\mathbf{x}) d\mathbf{x}.$$

$\rightarrow$ (weighted) circular/torical Radon transforms.

Radon transform on spindle tori

G. Rigaud and B. Hahn (2018) 3D Compton scattering imaging and contour reconstruction for a class of Radon transforms *Inverse Problems* 34 (2018) 075004 (22pp).

First-order scattering in 3D CSI [R. and Hahn (2018)]

Let $n_e \in L^2(\Omega)$ the electron density compactly supported on $\Omega \subset \mathbb{R}^3$. The **number of detected (first-order) scattered photons with energy** E_ω, g, is written

$$g_1(\mathbf{s}, \mathbf{d}, \omega) = \mathcal{T} n_e(\mathbf{s}, \mathbf{d}, \omega) := \int_{\mathbf{x} \in \mathfrak{T}(\omega, \mathbf{d}, \mathbf{s})} \frac{A_0(\mathbf{x})}{|\mathbf{x} - \mathbf{s}|^2} \frac{A_\omega(\mathbf{x})}{|\mathbf{x} - \mathbf{d}|^2} n_e(\mathbf{x}) d\mathbf{x}.$$

The phase function of the manifold $\mathfrak{T}(\omega, \mathbf{d}, \mathbf{s})$ is given by

$$\omega = \arctan \left(\frac{\sqrt{\|\mathbf{d} - \mathbf{s}\|^2 \|\mathbf{x} - \mathbf{s}\|^2 - ((\mathbf{x} - \mathbf{s}) \cdot (\mathbf{d} - \mathbf{s}))^2}}{(\mathbf{x} - \mathbf{s}) \cdot (\mathbf{d} - \mathbf{s}) - \|\mathbf{x} - \mathbf{s}\|^2} \right) \triangleq \phi(\mathbf{x}, \mathbf{d}, \mathbf{s}).$$

Rotation-free modalities on CSI

$g_1(\mathbf{s}, \mathbf{d}, \omega) = \mathcal{T} n_e(\mathbf{s}, \mathbf{d}, \omega)$ with $(\mathbf{d} - \mathbf{s}) \in \mathbb{V}$. But which $\mathbb{V}$?

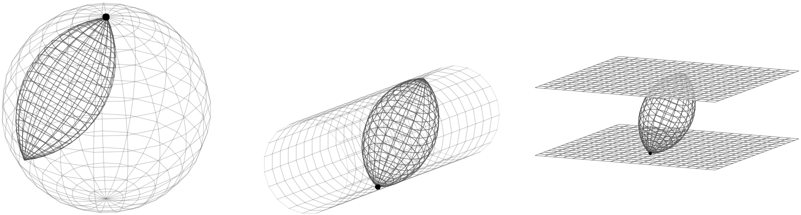

(a) (b) (c)

In 3D one can design the same concept as in 2D with various architectures:

(a) with detectors on a sphere,
(b) with detectors on a cylinder,
(c) with detectors on two planes.

Geometry of the second-order scattered radiation

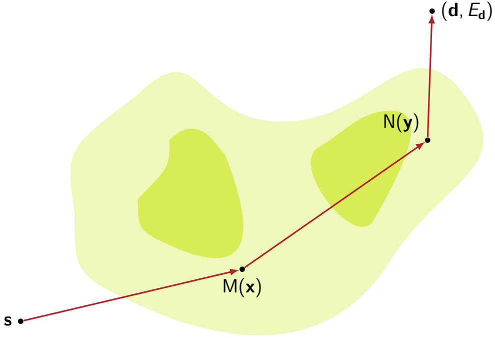

Geometry of the second-order scattered radiation

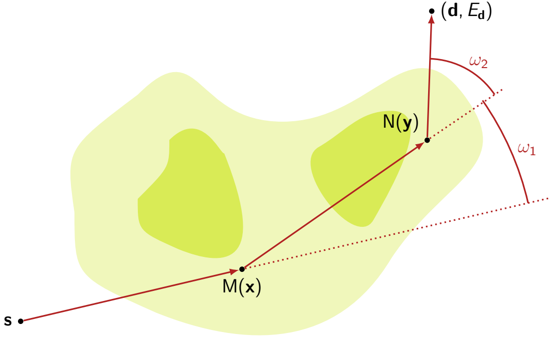

Due to the Compton Formula

$$\cos\omega_1 + \cos\omega_2 = 2 - mc^2\left(\frac{1}{E_{\mathbf{d}}} - \frac{1}{E_0}\right)$$

Geometry of the second-order scattered radiation

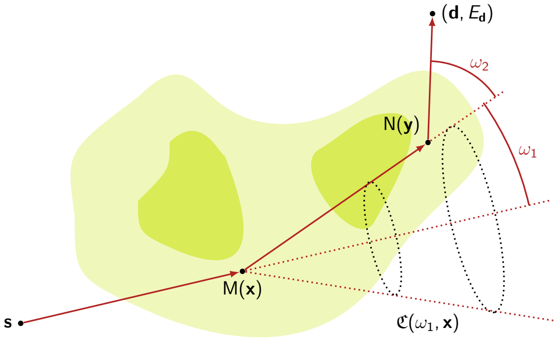

Due to the Compton Formula

$$\cos\omega_1 + \cos\omega_2 = 2 - mc^2\left(\frac{1}{E_\mathbf{d}} - \frac{1}{E_0}\right)$$

Geometry of the second-order scattered radiation

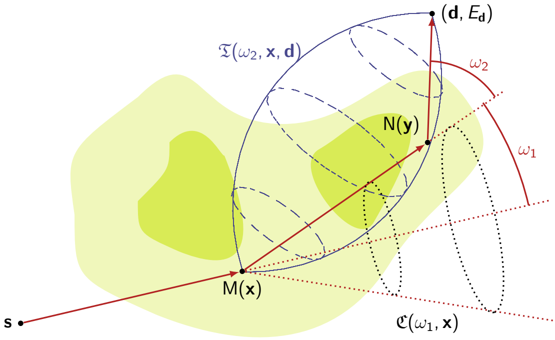

Due to the Compton Formula

$$\cos\omega_1 + \cos\omega_2 = 2 - mc^2\left(\frac{1}{E_{\mathbf{d}}} - \frac{1}{E_0}\right)$$

Geometry of the second-order scattered radiation

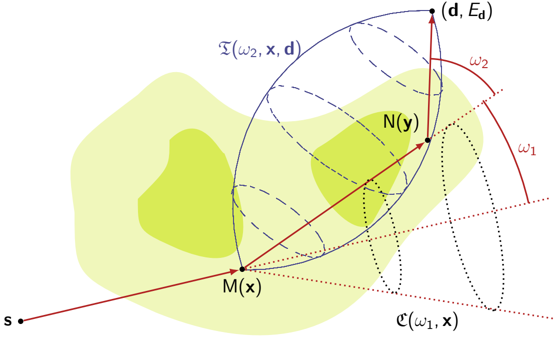

$$\mathbf{y} \in \mathfrak{C}(\omega_1, \mathbf{x}) \cap \mathfrak{T}(\omega_2, \mathbf{x}, \mathbf{d})$$

Due to the Compton Formula

$$\cos\omega_1 + \cos\omega_2 = 2 - mc^2\left(\frac{1}{E_{\mathbf{d}}} - \frac{1}{E_0}\right)$$

Characterizing the intersection

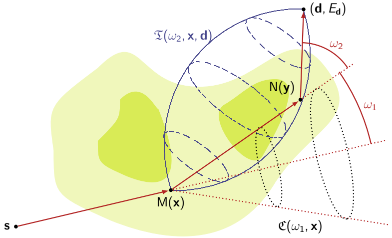

$$\mathbf{y}_\cap \in \mathfrak{C}(\omega_1, \mathbf{x}) \cap \mathfrak{T}(\omega_2, \mathbf{x}, \mathbf{d})$$

can be represented using parameters $(\omega_1, \varphi) \in [0, \pi] \times [0, 2\pi]$ by

$$\mathbf{y}_\cap = \mathbf{x} + r_\cap \, R_2 R_1 \begin{pmatrix} \sin\omega_1 \cos\varphi \\ \sin\omega_1 \sin\varphi \\ \cos\omega_1 \end{pmatrix} \quad \text{if } r_\cap > 0.$$

with

$$r_\cap := \|\mathbf{d} - \mathbf{x}\| \left(z_\cap - \frac{\sqrt{1 - z_\cap^2}}{\tan\omega_2} \right).$$

where

$$z_\cap := R_1(3,1) \sin\omega_1 \cos\varphi + R_1(3,2) \sin\omega_1 \sin\varphi + R_1(3,3) \cos\omega_1$$

An integral representation

Analytical formulation of g_2 [R'19]

Considering an electron density function $n_e(\mathbf{x})$ with compact support Ω, a monochromatic source $\mathbf{s}$ with energy E_0 as well as a detector $\mathbf{d}$ both located outside Ω. Then, the number of detected photons scattered twice arriving with an energy $E_{\mathbf{d}}$ are given by

$$g_2(\mathbf{d}, E_{\mathbf{d}}) = \int_\Omega \int_0^{2\pi} \int_0^{\pi} w_2(\mathbf{s}, \mathbf{x}, \mathbf{y}_\cap, \mathbf{d}, \omega_1, \varphi) n_e(\mathbf{x}) n_e(y_\cap) \mathrm{d}S_\cap(\omega_1, \varphi) \mathrm{d}\mathbf{x}$$

with the physical factors symbolized by

$$w_2(\mathbf{s}, \mathbf{x}, \mathbf{y}_\cap, \mathbf{d}, \omega_1, \varphi) = A_{E_0}(\mathbf{s}, \mathbf{x}) A_{E_{\omega_1}}(\mathbf{x}, \mathbf{y}_\cap) A_{E_{\omega_2}}(\mathbf{y}_\cap, \mathbf{d})$$

and the differential form of the intersection given by

$$\mathrm{d}S_\cap(\omega_1, \varphi) = r_\cap \sqrt{\sin^2 \omega_1 (r_\cap^2 + (\partial_{\omega_1} r_\cap)^2) + (\partial_\varphi r_\cap)^2}\, \mathrm{d}\omega_1 \mathrm{d}\varphi.$$

2 points spread function – Comparison with Monte-Carlo data

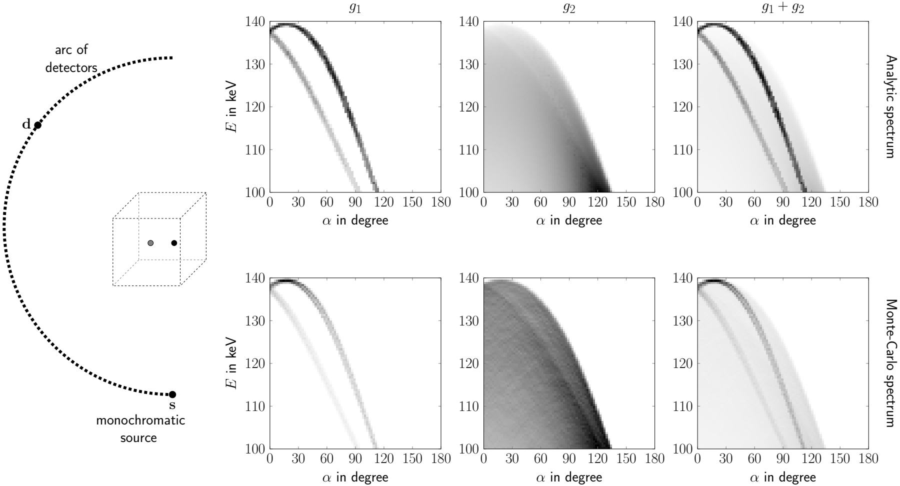

How to invert $\mathcal{T} n_e = g_1$?

$$\mathcal{T} n_e(\omega, \mathbf{s}, \mathbf{d}) = \int_{\mathbf{x} \in \mathfrak{T}(\omega, \mathbf{s}, \mathbf{d})} w(\mathbf{x}, \omega, \mathbf{s}, \mathbf{d}) n_e(\mathbf{x}) d\mathbf{x}$$

How to recover n_e ?

- Closed-form inversion formulae are unknown.
- Iterative algorithms (Landweber, Kaczmarz, etc) are expensive.

What about the contours n_e ?

- Microlocal analysis states the singularities of n_e are preserved through the data (Quinto, Webber and Holman 17).
- Beylkin (1984) proposed a study of the generalized Radon transform on a family of manifold and a class of reconstruction operators.

G. Beylkin (1984) The inversion problem and applications of the generalized Radon transform, Communications on Pure and Applied Mathematics, 37, 579–599.

P. Kuchment et al. (1995) On local tomography, Inverse Problems, 11, 571–589.

T. Quinto, V. Krishnan (2015) Microlocal Analysis in Tomography, in Handbook of Mathematical Methods in Imaging, 2e, Book editor: Otmar Scherzer.

J. Webber, S. Holman (2017) Microlocal analysis of a spindle transform, arXiv.

An extension of Beylkin's results

G. Rigaud and B. Hahn (2018) 3D Compton scattering imaging and contour reconstruction for a class of Radon transforms *Inverse Problems* 34 (2018) 075004 (22pp).

Given the generalized 3D Radon transform along $\phi \in \mathbb{M}$,

$$\mathcal{R}_c f(p,\theta) = \int_\Omega c(\mathbf{x},p,\theta)\; f(x)\; \delta(p - \phi(\mathbf{x},\theta)) d\mathbf{x}, \quad (p,\theta) \in \Pi \times \Theta,$$

and defining the following *backprojection* operator

$$\mathcal{R}_b^* g(\mathbf{y}) = \int_\Theta b(\mathbf{y},\theta)\; g(\phi(\mathbf{y},\theta),\theta)\; h(\mathbf{y},\theta) d\theta \quad \text{for} \quad \mathbf{y} \in \Omega.$$

Theorem [R. and Hahn (2018)]

Given $\mathcal{R}_c f = g$ with $f \in L^2(\Omega)$ and $c(\cdot)$ being a strictly positive C^∞ smooth function then,

$$\mathcal{K} f := \frac{-1}{8\pi^2} \mathcal{R}_b^* \partial_p^2 g = f + \mathcal{E} f$$

with $b(\mathbf{y},\theta) = (c(\mathbf{y},\phi(\mathbf{y},\theta),\theta))^{-1}$ and $\mathcal{E}$ a smoothing integral operator.

Contours reconstruction from

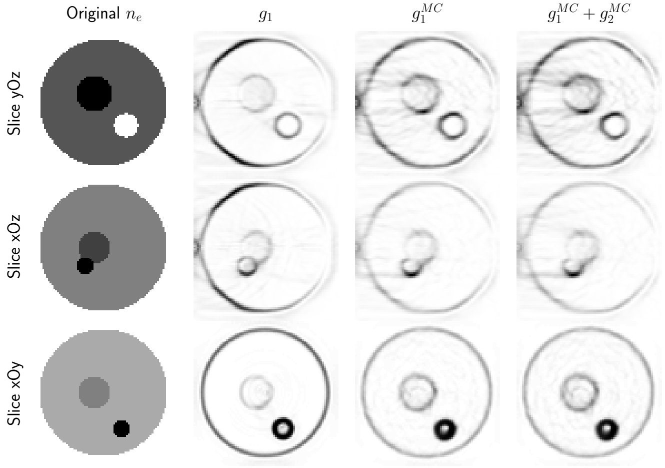

- **Our problem?**

$$g_1(\omega, \mathbf{s}, \mathbf{d}) = \mathcal{T} n_e(\omega, \mathbf{s}, \mathbf{d}) = \int_{\mathbf{x} \in \mathfrak{T}(\omega, \mathbf{s}, \mathbf{d})} w(\mathbf{x}, \omega, \mathbf{s}, \mathbf{d}) n_e(\mathbf{x}) d\mathbf{x}$$

is a non-linear mapping in n_e (w depends on n_e) since

$$a_E(x) \approx E^{-3} \mu_{PE}(x) + \sigma(E) n_e(x).$$

Continuity of g_1 [R'19]

Denoting by $\mathcal{T}_{\mathbf{d}}$, the restriction of $\mathcal{T}$ to one detector $\mathbf{d}$ and a given source $\mathbf{s}$, then $\mathcal{T}_{\mathbf{d}} : L_2(\Omega) \to L_2(\mathbb{R})$ is continuous

- **Idea:** approximate g_1 by

$$\mathcal{T}(f, n_e)(\omega, \mathbf{v}) = \int_\Omega \mathcal{W} n_e(\mathbf{x}, \omega, \mathbf{v}) \ f(\mathbf{x}) \ \delta(\omega - \phi(\mathbf{x}, \mathbf{v})) \ \mathrm{d}\mathbf{x}$$

with $n_e \in C^\infty(\Omega)$ and $f \in L_2(\Omega)$ such that $\|f - n_e\|_{L_2(\Omega)} \leq \epsilon \ll 1$.

Representation as Fourier integral operators

G. Rigaud (2019) 3D Compton scattering imaging: study of the spectrum and contour reconstruction, *arXiv:1908.03066*

Smoothness property of g_1 [R'19]

Let $n_e \in C^\infty(\Omega)$ given with Ω an open subset of $\mathbb{R}^3$. Then the operator $\mathcal{T}(\cdot, n_e)$ is a Fourier integral operator of order -1.

Smoothness property of g_2 [R'19]

Let $n_e \in C^\infty(\Omega)$ given with Ω an open subset of $\mathbb{R}^3$. Then, under some assumptions on the phase

$$\Psi(\mathbf{y}, \mathbf{x}, \mathbf{d}) := \psi(\mathbf{y}, \mathbf{x}) + \cos\left(\cot^{-1} \phi(\mathbf{y}, \mathbf{x}, \mathbf{d})\right),$$

g_2 can be understood as a Fourier integral operator of order $-\frac{7}{4}$.

F. Treves (1980) Introduction to pseudodifferential and Fourier Integral Operators, Plenum Press, New York, The University Series in Mathematics.

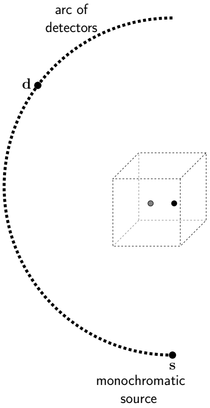
arc of
detectors
d
s
monochromatic
source

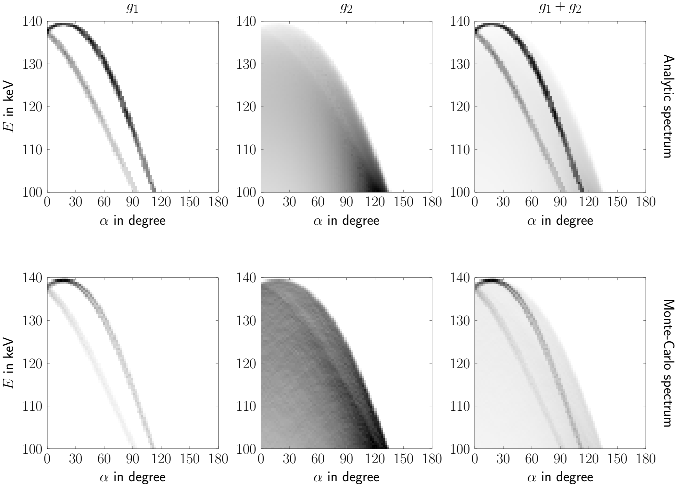
g_1
g_2
$g_1 + g_2$
E in keV
α in degree
Analytic spectrum
Monte-Carlo spectrum
140
130
120
110
100
0 30 60 90 120 150 180

Contours reconstruction from

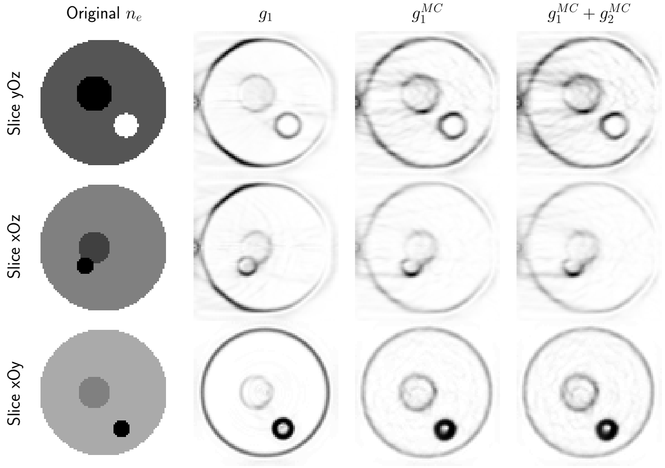

Outlook and Challenges

We learned

- how to model the first- and second-order scattering
- that the contours of the density can be extracted from the spectrum

Now we need

- better estimates for the smoothness properties
- to deal with limited data problems in CSI
- to deal with the polychromatic case
- iterative techniques

Outlook and Challenges

We learned

- how to model the first- and second-order scattering
- that the contours of the density can be extracted from the spectrum

Now we need

- better estimates for the smoothness properties
- to deal with limited data problems in CSI
- to deal with the polychromatic case
- iterative techniques

⇒ For a start: modified OSEM algorithm applied only on g_1

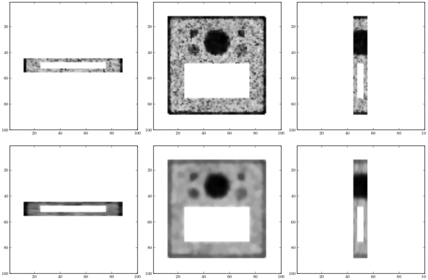

Some literature

- **G. Rigaud** (2013) On the inversion of the RT on a generalized Cormack-type class of curves, Inverse Problems, 29, 115010.
- **G. Rigaud** (2017) Compton Scattering Tomography: Feature Reconstruction and Rotation-Free Modality *SIAM J. Imaging Sci.*, 10(4), 2217-2249.
- **G. Rigaud** and B. Hahn (2018) 3D Compton scattering imaging and contour reconstruction for a class of Radon transforms *Inverse Problems* 34 (2018) 075004 (22pp).
- **G. Rigaud** and B. Hahn (2019) Reconstruction Algorithm for 3D Compton scattering imaging with incomplete data *Submitted*
- **G. Rigaud** (2019) 3D Compton scattering imaging: study of the spectrum and contour reconstruction, *arXiv:1908.03066*

Thank you
for your attention

Questions ?